Ultrafast tuning of two-dimensional planar photonic-crystal waveguides via free-carrier injection and the optical Kerr effect

Jessica P. Mondia, Hong Wee Tan, Stefan Linden,* and Henry M. van Driel

Department of Physics, University of Toronto, Toronto, Canada, M5S-1A7

Jeff F. Young

Department of Physics and Astronomy, Advanced Materials and Process Engineering Laboratory, University of British Columbia, Vancouver, British Columbia, Canada V6T-1Z1

Received March 4, 2005; revised manuscript received June 3, 2005; accepted June 9, 2005

Femtosecond pump–probe reflectivity and second-harmonic spectroscopy experiments are used to investigate the optical tuning of leaky modes in a two-dimensional GaAs photonic-crystal waveguide. For above bandgap excitation with 270 fs, 800 nm pulses with a pump fluence of 100 μJ cm^{-2}, a blueshift of 16±2 nm is measured for a 1900 nm leaky mode, as observed from the shift of the resonantly enhanced second-harmonic pulse. Theoretical calculations of carrier-induced changes in the refractive index from band filling, bandgap shrinkage, and Drude contributions are in good agreement with the results. Recovery occurs within 2 ps and is attributed to recombination via deep-centered defects. For below bandgap excitation with 166 fs, 1900 nm pulses with a fluence of 800 μJ cm^{-2}, redshifts $\geqslant$1.5 nm of the 1360 nm leaky mode are induced via the optical Kerr effect during the early part of the pump pulse, but thereafter the mode is blueshifted, owing likely to free carriers injected into or from deep-centered defects.

OCIS codes: 190.5970, 320.7110.

1. INTRODUCTION

All-optical tuning of semiconductor photonic crystals on a femtosecond–picosecond time scale can lead to new applications for photonic crystals, such as all-optical switching or signal processing. A number of different proposals and experimental demonstrations have emerged over the past decade. The most promising mechanism for ultrafast tuning involves optically inducing of changes in the refractive index of one or both of the constituents of a photonic crystal via free-carrier injection,[1–5] the optical Kerr effect,[3,5,6,7] or the optical Stark effect.[8] In this paper comprehensive femtosecond pump–probe second-harmonic (SH) and reflectivity experiments are employed to characterize the roles of free carriers and the optical Kerr effect in tuning leaky eigenmodes of a GaAs planar photonic-crystal waveguide (PPCW). We have observed tuning by as much as 16 nm.

Two types of experiment have been performed. In the first, 800 nm, 270 fs pump pulses with photon energy ($\hbar\Omega \approx 1.55$ eV) slightly above the electronic bandgap ($E_g = 1.42$ eV at 295 K) of GaAs are used to inject free carriers into the GaAs backbone in order to modify the properties of the PPCW leaky modes. However, in contrast to previous studies that probed changes in leaky or bound modes using reflectance techniques,[4] we have used SH generation to measure changes in leaky modes. The SH light, which becomes spectrally narrow and enhanced when either the incoming fundamental beam or the outgoing SH beam resonantly couples[9,10] to a leaky mode of the PPCW, is a more precise diagnostic of leaky modes. This is demonstrated using 166 fs, 1900 nm ($\hbar\Omega \approx 0.65$ eV) fundamental pulses incident at particular angles on the PPCW. By using the SH technique with a broadband fundamental pulse (with a bandwidth of 70 nm), the tuning of different modes can also be monitored simultaneously. The leaky mode tuning is well described by simulations that include three free-carrier contributions to the refractive index; these are the Burstein–Moss shift of interband transitions (related to band filling), Drude contributions, and bandgap renormalization (shrinkage).[11] From time-resolved reflectivity experiments at 1900 nm, the refractive-index change is measured to decay in ~2 ps, which we attribute to a free-carrier lifetime.

In the second set of experiments, the PPCW is optically pumped with 1900 nm pulses (i.e., below $E_g/2$) in order to utilize the Kerr nonlinearity to tune leaky modes and obtain a pulse-width-limited response. Earlier, Banaee *et al.*[12] proposed a method to engineer a two-dimensional (2-D) GaAs PPCW to obtain leaky modes with large-quality (Q) factors and thus enhance the optical Kerr effect. Here, evidence for such an enhancement is presented. However, besides Kerr-induced contributions to refractive-index changes, we also observe Drude-related effects associated with carriers excited via single- or multiphoton processes from deep-centered defects in the processed GaAs backbone.

2. EXPERIMENTAL DETAILS

Our waveguide structure was previously described by Mondia *et al.*,[9] where it was used to demonstrate en-

hanced SH generation via leaky modes. As shown in Fig. 1, the structure consists of a square lattice of air holes etched through a 140 nm thick layer of GaAs, grown in the ⟨100⟩ direction, and supported on a ~1 μm thick Al_2O_3 cladding layer. The air-pore diameter and lattice spacing are 320 and 770 nm, respectively. The 90 μm × 90 μm sample was fabricated with conventional electron-beam lithography and plasma-etching techniques.[13,14]

The pump–probe measurements were performed with pulses from an optical parametric amplifier pumped by a 130 fs, 800 nm Ti:sapphire regenerative amplifier with a pulse repetition rate of 250 kHz. The signal and idler beams from the parametric source consisted of 130 fs pulses tunable in the range of 1.2–2.0 μm. Nondegenerate pump–probe pulses were incident collinearly along a plane defined by the sample normal and the $\Gamma-X$ photonic crystal direction for different angles of incidence (θ), as shown in Fig. 1. Spectra of the probe reflectivity and the SH emission in the specular direction were measured with a monochromator and a PbS and a liquid-nitrogen-cooled InGaAs detector, respectively. Time-resolved pump–probe measurements were performed with a variable delay stage installed in the pump beam path.

Figure 2 shows the calculated dispersion curves[9,10] for the relevant leaky modes in the SH experiment. The solid curve represents the *s*-polarized leaky mode (at twice its energy) with which the incoming fundamental couples, and the dashed curves represent the *p*-polarized leaky modes with which the outgoing SH couples. In the figure, for light of wavelength λ, the in-plane component of the light wavevector, viz., $k_{\parallel}=2\pi/\lambda \sin(\theta)$, is represented by the experimental variable parameter θ. When the PPCW is illuminated by *s*-polarized 1900 nm light at $\theta \simeq 28°$ or $\theta \simeq 37°$, the fundamental beam couples to the lowest-order leaky photonic eigenmode, *and* the *p*-polarized SH field (phase matched to the fundamental) also couples to another leaky eigenmode, producing a double-resonance condition.[9,10] In general, carrier-induced changes to the refractive index alter the dispersion diagram and hence shift the *p*-polarized SH spectra.

To perform above-bandgap excitation of the PPCW, the unconverted 800 nm pulse energy from the parametric

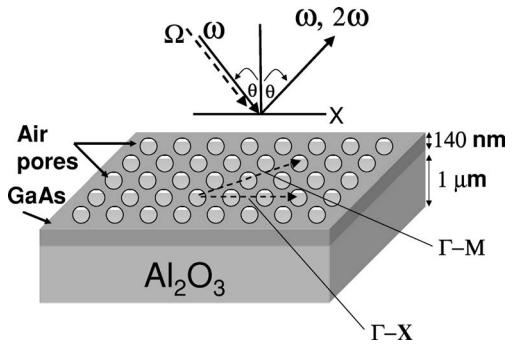

Fig. 1. Schematic diagram of the planar photonic-crystal waveguide. The diameter of the air pores in the GaAs are 320 nm, and the distance between adjacent pores is 770 nm. The $\Gamma-X$ and $\Gamma-M$ directions of the photonic crystal are illustrated with arrows. Also illustrated is the beam geometry used to monitor changes to either the reflectivity or the SH spectra for a collinear pump beam at frequency Ω.

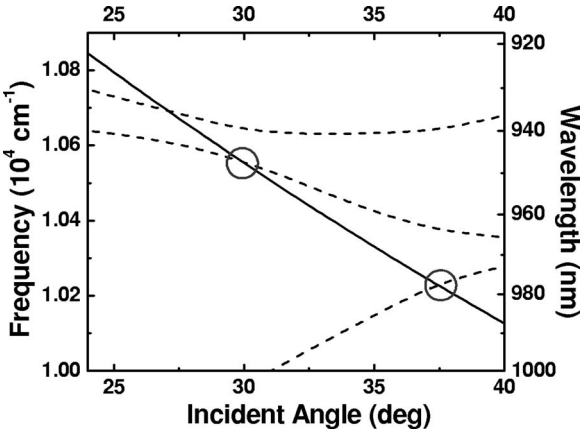

Fig. 2. PPCW dispersion curves for the leaky modes used in the SH studies; the in-plane wavevector is represented by the angle of incidence θ. The solid curve represents the lowest order *s*-polarized photonic band (to which a fundamental beam is coupled), and the dashed curve shows the *p*-polarized photonic band to which a SH beam can couple. To illustrate where phase matching can occur, the *s*-polarized band is plotted at twice its frequency and twice its wavevector. Circles represent locations of peak SH enhancement related to a double-resonance condition.

amplifier was used to inject free carriers in the PPCW with a focused spot size (FWHM) of 66 μm. Collinearly incident 1900 nm *s*-polarized pulses were focused to a spot size of 30 μm (FWHM) on the sample and at the center of the pump spot. The peak fluence of the 1900 nm beam was $<300\ \mu J\ cm^{-2}$, while the 800 nm pump fluence was varied between 0 and 100 $\mu J\ cm^{-2}$. SH spectra were obtained for several angles of incidence in the range $24° < \theta < 38°$ for a pump–probe delay of ~200 fs, yielding the maximum SH signal.

To perform below-bandgap excitation intended to reveal Kerr-related tuning, *s*-polarized 1900 nm pump pulses were used to resonantly induce a shift in the 1360 nm leaky mode (not shown in Fig. 2). The transient response of the *p*-polarized 1360 nm leaky mode excited at $\theta=28°$ was measured for 1900 nm pump pulse fluences up to 800 $\mu J\ cm^{-2}$. To avoid probe-induced carriers contributing to the refractive-index change (e.g., activated from defects as discussed below), the 1360 nm probe-beam peak fluence was $<2\ nJ\ cm^{-2}$. The pump and probe spot sizes were 55 and 26 μm (FWHM), respectively.

3. THEORETICAL CONSIDERATIONS

For our experiments refractive-index changes can be induced via excitation of real carriers or virtual carriers, with the latter leading to the Kerr effect. We consider the first excitation of real carriers. There are three mechanisms by which free carriers can induce changes to a semiconductor's refractive index. These include contributions from the Drude effect, band filling, and bandgap shrinkage. In the high-frequency limit, the Drude contribution to the real part of the refractive index is given by[11]

$$\Delta n = -\frac{e^2 N}{2n\epsilon_0 m^* \omega^2}, \tag{1}$$

where N is the electron-hole pair density, ω is the probe frequency, e is the electron charge, ϵ_0 is the permittivity of

free space, n (=3.6 for GaAs at the probe wavelength) is the quiescent refractive index, and m^* is the optical effective mass. The initial carrier density can be related to the incident pump–pulse intensity I_Ω, material reflectivity, and absorption coefficient in the usual manner.[15] In what follows we ignore carrier diffusion for relatively uniform excitation of the GaAs; carrier evolution is therefore determined by electron-hole recombination. For 800 nm, 270 fs pulse excitation at our peak fluence of $\sim 100\ \mu\mathrm{J\ cm^{-2}}$, we estimate $N \leqslant 5\times 10^{18}\ \mathrm{cm^{-3}}$.

The Drude model is a good approximation for probe photon energies $\hbar\omega \ll E_g$. However, for probe energies near E_g, as in our case, contributions associated with interband transitions such as band filling and bandgap shrinkage also need to be considered.[11] For a direct bandgap semiconductor such as GaAs, the change in the absorption coefficient due to band filling can be described by

$$\Delta\alpha_{\mathrm{bf}}(\omega,N) = -\sum_i \alpha_0^i [f_e^i(\omega,N) + f_h^i(\omega,N)],$$

where $f_e^i(\omega,N)$ and $f_h^i(\omega,N)$ are the Fermi occupancy factors for the optically coupled electron and hole states at the photon energy $\hbar\omega$, respectively, and the summation is over the heavy hole (hh) and light hole (lh) valence bands. The quiescent optical absorption coefficient associated with the different hole bands and for $\hbar\omega \geqslant E_g$ is given by

$$\alpha_0^i = \frac{C_i}{\hbar\omega}(\hbar\omega - E_g)^{1/2}, \tag{2}$$

where the constants C_i are obtained by fits to experimental data.[11]

Based on empirical data, the bandgap shrinkage (renormalization) for large carrier densities ($N > 7\times 10^{16}\ \mathrm{cm^{-3}}$) is given by

$$\Delta E_g(N) \approx -\frac{\kappa}{n^2}N^{1/3}, \tag{3}$$

where $\kappa = 3.15\times 10^{-7}$ eV cm for GaAs. The corresponding change in the absorption coefficient is thus given by

$$\Delta\alpha_{\mathrm{br}}(\omega,N) = \frac{C_{\mathrm{hh}} + C_{\mathrm{lh}}}{\hbar\omega}\{[\hbar\omega - E_g - \Delta E_g(N)]^{1/2} - (\hbar\omega - E_g)^{1/2}\}, \tag{4}$$

where only heavy-hole and light-hole valence bands are considered for our photon energies. The contributions to the change in the refractive index Δn from bandfilling (bf) and bandgap shrinkage–renormalization (br) can then be obtained through the Kramers–Kronig relations

$$\Delta n_{\mathrm{bf,br}}(\omega,N) = \frac{c}{\pi}\mathcal{P}\int_0^\infty \frac{\Delta\alpha_{\mathrm{bf,br}}(\omega',N)}{\omega'^2 - \omega^2}\mathrm{d}\omega', \tag{5}$$

where $\mathcal{P}$ refers to the principal part of the integral.

Figure 3 shows Δn as a function of probe photon energy $\hbar\omega$ for band filling, bandgap shrinkage, and Drude contributions for an electron-hole density of $10^{18}\ \mathrm{cm^{-3}}$ and at room temperature. The total index change is obtained by adding the three contributions, which are assumed to be independent at our densities ($N < 5\times 10^{18}\ \mathrm{cm^{-3}}$). For $\hbar\omega \sim E_g$, band-filling and bandgap-shrinkage effects dominate, but for $\hbar\omega \ll E_g$ Drude contributions play a larger role in determining the value of Δn. Since the total index change is always negative for the probe energies used in the experiments ($0.63 < \hbar\omega < 1.3$ eV), the leaky modes are expected to be blueshifted following injection of electron-hole pairs.

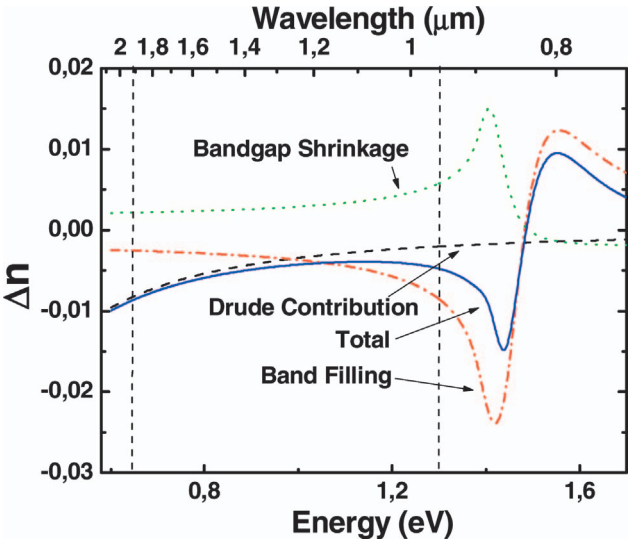

Fig. 3. Calculated changes in the index of refraction induced by electron-hole pairs in GaAs as a function of probe-photon energy; contributions from bandgap shrinkage, Drude, and band-filling mechanisms are illustrated for an electron-hole density $N = 1\times 10^{18}\ \mathrm{cm^{-3}}$. The vertical dashed lines represent the boundaries of the energy regime experimentally probed.

For below-bandgap excitation ($\hbar\Omega < E_g$) the optical Kerr effect is expected to dominate changes in the refractive index. However, if carriers are generated via single- or multiphoton absorption (possibly with defects assisting), then index changes from one or more of the mechanisms outlined above may occur. For the Kerr effect in our experiment, the change in the refractive index experienced by the probe beam at ω in the presence of a pump beam at Ω is given by[16]

$$\Delta n(\omega) = 2\ \mathrm{Re}[\chi^{(3)}(\omega;\omega,-\Omega,\Omega)E(\Omega)E^*(\Omega)]/2n = 2n_2 I_\Omega, \tag{6}$$

where $\chi^{(3)}$ is a third-order optical susceptibility and n_2 is the nonlinear refractive index. It is possible that a cascaded $\chi^{(2)}$ process may also contribute to the overall induced change in the refractive index[17]; however, this effect is likely negligible since the optical interaction length in the PPCW is small and the leaky mode quality factor is low ($Q \sim 50$).

In principle, thermal effects can also contribute to a change in the refractive index. However for GaAs[18] $\mathrm{d}n/\mathrm{d}T = 2.64\times 10^{-4}\ \mathrm{K^{-1}}$ and since the sample temperature rise is $\ll 1$ K per pulse, thermally induced changes to the refractive index are approximately 2–3 orders of magnitude smaller than the changes due to band filling and Drude contributions. Moreover, no accumulated pulse effects were observed in the measured transient-response traces. Thus thermal effects have been neglected.

Simulations of the change in reflectivity of the PPCW as a function of change in GaAs refractive index were car-

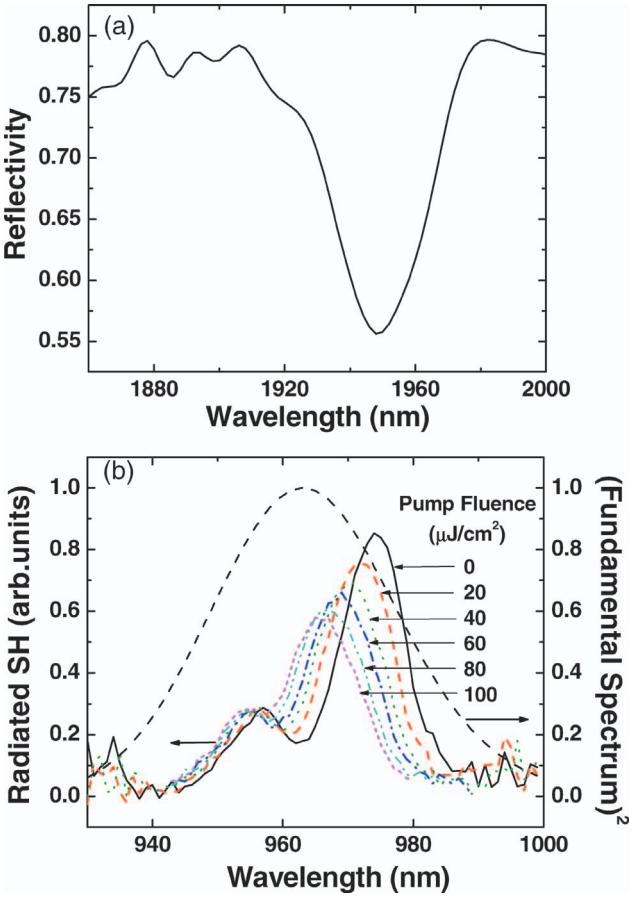

Fig. 4. (a) Reflectivity spectrum of a 1900 nm *s*-polarized pulse at $\theta=34°$; (b) *p*-polarized SH spectra at $\theta=34°$ for different 800 nm pump pulse fluences. Also shown is the square of the 1900 nm pump spectrum plotted at half its wavelength.

ried out using a scattering matrix method (SMM) developed by Whittaker and Culshaw.[19] The wavelength shift of different leaky modes was determined by noting the spectral dependence of the leaky mode for different carrier densities and refractive indices.

4. TUNING OF MODES: $\hbar\Omega > E_g$

Figure 4(a) shows the normalized reflectivity spectrum of the PPCW for *s*-polarized 1900 nm fundamental pulses incident at $\theta=34°$. The dip in the reflectivity spectrum is indicative of a leaky mode of the PPCW.[13] Figure 4(b) shows the corresponding *p*-polarized SH spectra for different 800 nm pump fluences for the beam geometry shown in Fig. 1 ($\theta=34°$). Owing to beam focusing, the spread of θ for the 1900 nm pulses is about ±2°; this accounts for the large (10 nm) SH bandwidth compared with the (2 nm) SH bandwidth calculated for plane-wave excitation. Also shown in the figure is the square of the 1900 nm pulse spectrum at half the wavelength. Because of the broad spectral bandwidth (~70 nm) of the 1900 nm pulse, two SH peaks are observed. The first peak at ~955 nm is associated with the outgoing SH field coupling resonantly to a leaky mode of the PPCW. The second peak at ~975 nm [half the wavelength of the resonant feature observed in Fig. 4(a)] occurs because the incoming 1900 nm beam couples resonantly to a leaky mode of the PPCW.[9] As the pump fluence increases, the SH spectra shift to shorter wavelengths. The direction of the shift is in agreement with tuning via free-carrier injection. The slight decrease in the 975 nm peak amplitude as the pump fluence is increased is most likely a consequence of tuning the photonic bands away from the double-resonance condition (see Fig. 2 for $\theta=37°$).[9]

The sharp SH peaks were fitted with either a single or double Gaussian function to ascertain the peak wavelengths. Owing to the low SH signal associated with a coupling of the outgoing SH pulse to broad resonant modes, SH spectra with double-peaked profiles were observed for only $\theta>32°$. Figure 5(a) gives the peak position of the SH signal associated with the incoming fundamental beam coupled resonantly to a mode of the PPCW for different θ and for different pump fluences. The solid curves are best fits for measurements with the same pump fluence. The data illustrate that the fundamental 1900 nm mode shifts uniformly toward shorter wave-

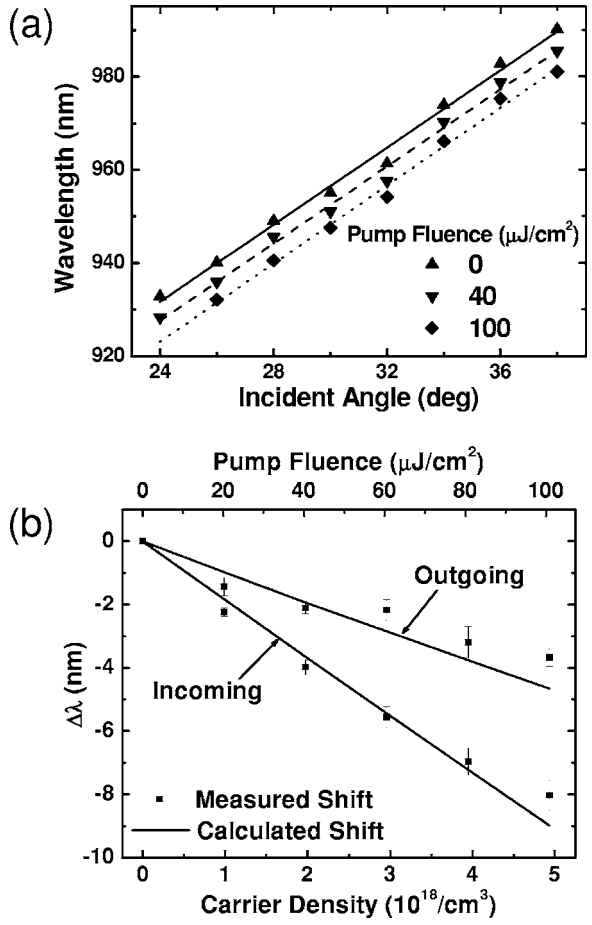

Fig. 5. (a) Peak spectral position associated with the incoming 1900 nm pulses resonantly coupled to a mode of the PPCW for different θ and 800 nm pump fluences. The lines of best fit represent the SH photonic bands for different pump fluences. (b) The dependence of the SH blueshift on carrier density (pump fluence) for leaky modes associated with the incoming fundamental beam and the outgoing SH beam resonant with different leaky modes of the PPCW. Each data point represents the average shift over all measured θ. The solid curves are calculated shifts incorporating band-filling effects, bandgap shrinkage effects, and Drude contributions.

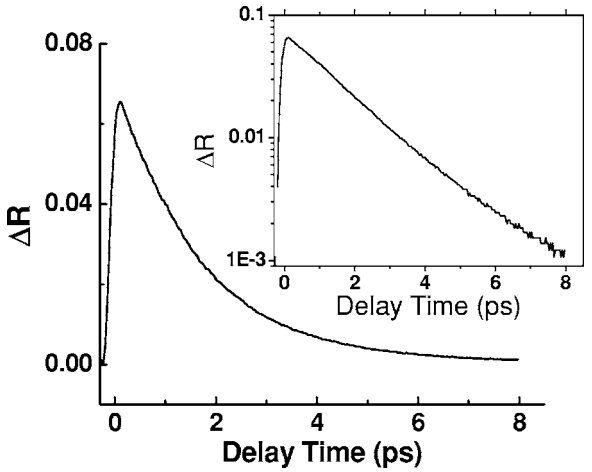

Fig. 6. Transient response of the 1900 nm leaky mode for a 800 nm pump fluence of 100 μJ/cm^2 and incident angle θ=28°. The inset represents the same data on a semilog plot. Similar measurements were made for other angles, yielding an average decay time of approximately 2 ps.

lengths as the pump fluence increases. This observation is in agreement with theory that predicts that the lowest-order *s*-polarized photonic band, for $10° < \theta < 50°$, shifts uniformly for an induced index change <0.01 in the GaAs backbone; this is an upper bound for our experimental shift. An SH wavelength shift of -8 ± 1 nm (the average value recorded for $24° < \theta < 38°$) was obtained for a pump fluence of 100 μJ cm^{-2}; this implies a blueshift of the 1900 nm leaky mode of 16 ± 2 nm. From Fig. 5(a) the 955 nm peak clearly shifts less than the 975 nm peak. This is illustrated more clearly in Fig. 5(b), which shows the SH shift as a function of pump fluence for either the incoming fundamental (1900 nm) beam or the outgoing SH (950 nm) beam resonant with a leaky mode of the PPCW. The data represent the shift averaged over all measured angles for a given pump fluence. The average blueshift of the outgoing SH beam for θ=34°, 36°, and 38° and for a pump fluence of 100 μJ cm^{-2} was determined to be 3.8 ± 0.3 nm.

This difference in the shift between the incoming fundamental and outgoing SH spectrum is due to the different mechanisms responsible for the index change at the different wavelengths. The mode with which the incoming beam couples is affected mainly by Drude contributions, whereas the mode with which the SH couples shifts as a result of all three carrier contributions. The solid curves in Fig. 5(b) represent the results of calculations based on the free-carrier model discussed earlier. The simulations assume that the GaAs portion of the PPCW was pumped uniformly, since the 800 nm pump beam was not resonant with a leaky mode. From the pump intensity and the sample reflectivity, the carrier density N was determined and hence the total change in the refractive index from carrier contributions [Eqs. (1) and (5)] was calculated. The shift of the leaky mode was then modeled using the SMM with the new refractive index as the input parameter for the GaAs backbone. A comparison between the experimental shift as a function of pump fluence (carrier density) and the simulated carrier-density dependence of the shift agree within the 10% experimental uncertainty. The small difference between theory and experiment at large fluences is most likely a consequence of band filling effects, i.e., energy states up to 0.13 eV ($\approx E_g - \hbar\Omega$) above the conduction-band minimum becoming filled, as expected at approximately 3×10^{18} cm^{-3}.

The ultrafast response of the sample, determined from the reflectivity of the 1900 nm pulse following 800 nm pulsed excitation for θ=28°, is shown in Fig. 6. The turn-on time is pulse-width limited, and the e^{-1} relaxation time is approximately 2 ps. The short carrier lifetime most likely results from enhanced surface recombination in the processed PPCW.[4] However, additional recombination mechanisms related to bulk defects in our samples are also expected to be important, since the observed recovery is not strictly exponential.[20] These defects may have been created in the fabrication processes.

5. TUNING OF MODES: $\hbar\Omega \ll E_g$

We now consider tuning of the PPCW when the pump photon energy $\hbar\Omega < E_g/2$. Figure 7(a) shows the time-resolved reflectivity of 1360 nm probe pulses for different 1900 nm pump fluences. The inset shows the correspond-

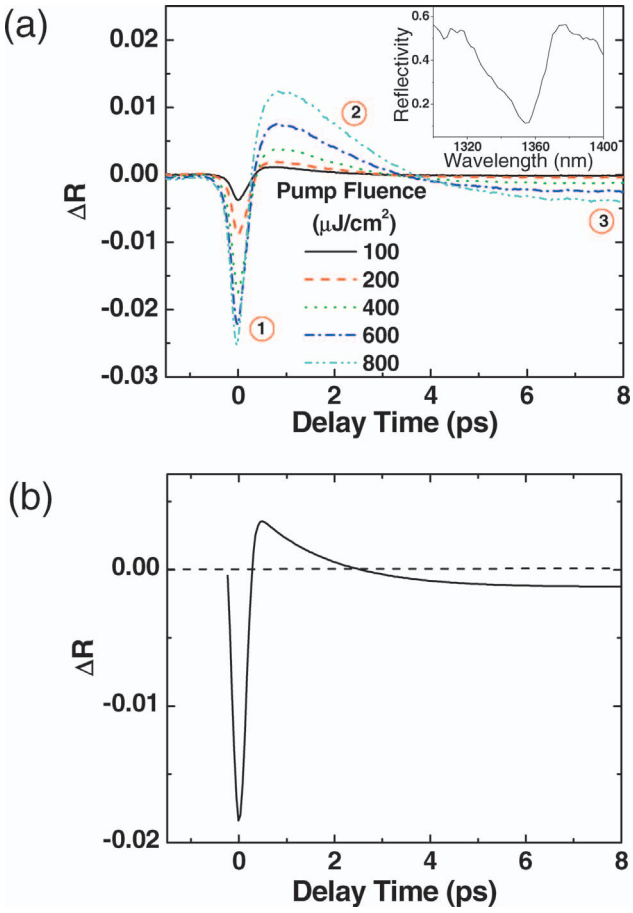

Fig. 7. (a) Transient response traces of the 1360 nm leaky mode for different 1900 nm pump fluences when both pump and probe beams are collinear and incident at θ=28°. Inset, spectrum of the 1360 nm probe reflectivity in the absence of the pump beam. (b) Simulations of the experimental results for an incident pump fluence of 400 μJ cm^{-2} using a Gaussian and two exponential functions.

ing 1360 nm probe reflectivity spectrum in the absence of the pump beam. On the long wavelength edge of this feature a negative or positive change in the reflectivity (ΔR) corresponds to a shift of the leaky mode to longer or shorter wavelengths, respectively. The initial negative dip (region 1) occurs on a time scale comparable with the cross-correlation width of the pump and probe pulses. The reflectivity subsequently reaches a positive peak before again decaying to negative values with a characteristic time of 2 ps (region 2). The final negative component (region 3) was observed to continue for at least several hundred picoseconds.

The transient response traces observed in Fig. 7(a) were fitted to a Gaussian plus two exponential functions of the form

$$\Delta R = f_1 \exp(-t^2/\tau_1^2) + f_2 \exp(-t/\tau_2) + f_3 \exp(-t/\tau_3). \quad (7)$$

Figure 7(b) shows the best fit for experiments conducted with an incident fluence of 400 μJ cm^{-2} and for which $f_1 = -2.4\times10^{-3}$, $f_2 = 7\times10^{-3}$, $f_3 = -1.5\times10^{-3}$, $\tau_1 = 212$ fs, $\tau_2 = 2$ ps, and $\tau_3 = 500$ ps. The simulated traces in all cases fit the experimental results quite well, and it was therefore possible to suggest that three different mechanisms were responsible for the temporal evolution of the reflectivity.

The pulse-width-limited response of region 1 is characteristic of a Kerr-like nonlinearity. At low pump fluence, the reflectivity change varies linearly with pump intensity, consistent with Eq. (6). At higher pump intensities there is a deviation from linearity owing to the competing mechanism associated with region 2. For a 1900 nm pump fluence of 800 μJ cm^{-2}, a maximum redshift of 1.5 nm was observed. The change in the reflectivity ΔR can be related to the index change by[5]

$$\Delta R = \frac{d\lambda}{dn}\frac{dR}{d\lambda}\Delta n, \quad (8)$$

where $d\lambda/dn = 307$ nm is the wavelength shift of the 1360 nm leaky mode as a function of index change (calculated from simulations), and $dR/d\lambda = -20$ μm^{-1} (taken from the measured reflectivity spectrum for the 1360 nm pulse). Assuming uniform pumping of the GaAs, accounting for the material reflectivity but neglecting defect related absorption effects, we conservatively estimate n_2 to be $(5\pm1)\times10^{-4}$ cm^2 GW^{-1}. This is within a factor of 2 of the bulk, calculated value[21] $n_2 = 3\times10^{-4}$ cm^2 GW^{-1}. The n_2 determinations for PPCWs with larger air-filling fractions might be more sensitive to the field distribution.[22] Regardless, we clearly observe an enhancement effect when the pump-beam wavelength was tuned from 1900 nm (on-resonance) to 2000 nm (off-resonance) while the probe-beam wavelength was kept centered at 1360 nm. The transient features of the traces were qualitatively the same, but the magnitude of the Kerr-induced shift was at least 6 times larger when the pump beam was on-resonance.

In region 2 of Fig. 7 the positive change for ΔR and the $\sim$2 ps temporal-response time in Fig. 7 is consistent with a real carrier excitation process. In particular, the sign and decay time agree well with the results obtained using excitation with $\hbar\Omega > E_g$. For a pump photon energy $\hbar\Omega = 0.65$ eV, free carriers could be generated in cold, clean GaAs via three-photon absorption. However, the fluence dependence of the reflectivity in region 2 as shown in Fig. 8 reveals a linear dependence at low pump fluence and a quadratic dependence at larger fluence. Since no cubic dependence was observed, the contribution from three-photon absorption processes is taken to be negligible. The carriers are most likely injected into and taken out of various defect states through single-photon absorption at low pump fluence and then through two-photon absorption or cascaded single-photon absorption processes at larger fluence, with defects playing a role. Supporting this argument is the steady increase in the decay time with increasing pump fluence (shown in the inset of Fig. 8), which is likely due to a partial saturation of defect states.[20]

The changes in reflectivity observed in region 3 are also likely a result of carrier trapping into or via defects. The redistribution of carriers into defect states, i.e., trapped at energy levels that lie within the bandgap, alters the linear optical susceptibility and hence changes the refractive index. It is difficult to deduce the exact mechanism behind the free-carrier generation or the long-lived process without further sample characterization. However, it is clear that these effects are not related to the photonic-crystal properties per se but are most likely due to alteration of the GaAs in the 2-D PPCW fabrication process.

6. CONCLUSIONS

We have shown qualitatively and quantitatively how femtosecond pulse excitation can reveal different optically induced tuning mechanisms of a 2-D GaAs photonic crystal waveguide for pump energies above and below the electronic bandgap of GaAs. The sharp SH spectra provide a sensitive technique for monitoring the tuning of PPCW modes. In addition, the large bandwidth of the input pulses (up to $\sim$70 nm) make it possible to observe the tuning of both the resonantly coupled incoming fundamental beam and the outgoing SH beam. The average shift of the two leaky modes are respectively -16 ± 2 nm and -3.8 ± 0.3 nm for a pump fluence of 100 μJ cm^{-2}. The

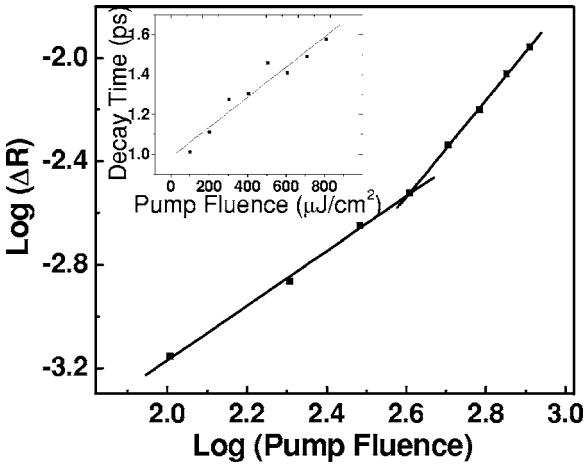

Fig. 8. Power dependence of $|\Delta R|$ for region 2 in Fig. 6. The data was fit to two straight lines with slope=1 and slope=1.9. Inset, decay time of data for region 2 as a function of 1900 nm pump fluence. Solid curve is best fit to the data.

difference between the average shifts is attributed to refractive-index changes from wavelength-dependent processes associated with band filling, bandgap shrinkage, and Drude effects. In principle, the amount of tuning also depends on how the spatial profile of the induced refractive-index change overlaps a particular eigenmode's field structure. However, for the cases considered here in which we most likely have spatially uniform refractive-index changes induced in the GaAs, this effect is not observable.

For pump energies below the bandgap three different temporal behaviors were observed for a resonantly coupled 1360 nm probe pulse. There is an initial pulse-width-limited decrease in the reflectivity owing to a nondegenerate Kerr effect. Subsequently, the reflectivity increases and decreases within a few picoseconds before it turns and remains negative for >100 ps. These longer temporal response effects are attributed to carriers injected into, taken out of, or trapped by defect and–or surface states. Evidence for an enhancement in the optical Kerr effect is observed when the PPCW is pumped via a leaky mode. However, the mode-quality factor and absorption from defect or surface states limit the enhancement in our particular sample.

ACKNOWLEDGMENTS

J.P.M. and H.M.v.D. gratefully acknowledge the financial support of Photonics Research Ontario and the Sciences and Engineering Research Council (SERC) of Canada as well as J. Sipe for many useful discussions and D. Whittaker for use of the SMM program. J.F.Y. acknowledges support from SERC and the Canadian Institute for Advanced Research.

Corresponding author H. M. van Driel can be reached at vandriel@physics.utoronto.ca

*Present address: Univ. Karlsruhe TH, Inst. Angew. Phys., Karlsruhe, D-76131 Germany.

REFERENCES

1. S. W. Leonard, H. M. van Driel, J. Schilling, and R. B. Wehrspohn, "Ultrafast band-edge tuning of a two-dimensional silicon photonic crystal via free-carrier injection," Phys. Rev. B **66**, 161102(R) (2002).
2. D. A. Mazurenko, R. Kerst, J. I. Dijkhuis, A. V. Akimov, V. G. Golubev, D. A. Kurdyukov, A. B. Pevtsov, and A. V. Sel'kin, "Ultrafast optical switching in three-dimensional photonic crystals," Phys. Rev. Lett. **91**, 213903 (2003).
3. A. Haché and M. Bourgeois, "Ultrafast all-optical switching in a silicon-based photonic crystal," Appl. Phys. Lett. **77**, 4089–4091 (2000).
4. A. D. Bristow, J.-P. R. Wells, W. H. Fan, A. M. Fox, M. S. Skoinick, D. M. Whittaker, A. Tahraoui, T. F. Krauss, and J. S. Roberts, "Ultrafast nonlinear response of A1GaAs two-dimensional photonic crystal waveguides," Appl. Phys. Lett. **83**, 851–853 (2003).
5. H. W. Tan, H. M. van Driel, S. L. Schweizer, R. B. Wehrspohn, and U. Gösele, "Nonlinear tuning of a two-dimensional silicon photonic crystal," Phys. Rev. B **70**, 205110 (2004).
6. X. Hu, Q. Zhang, Y. Liu, B. Cheng, and D. Zhang, "Ultrafast three-dimensional tunable photonic crystal," Appl. Phys. Lett. **83**, 2518–2520 (2003).
7. H. Inouye and Y. Kanemitsu, "Direct observation of nonlinear effects in a one-dimensional photonic crystal," Appl. Phys. Lett. **82**, 1155–1157 (2003).
8. M. Shimizu and T. Ishihara, "Subpicosecond transmission change in semiconductor-embedded photonic crystal slab: toward ultrafast optical switching," Appl. Phys. Lett. **80**, 2836–2838 (2002).
9. J. P. Mondia, H. M. van Driel, W. Jiang, A. R. Cowan, and J. F. Young, "Enhanced second-harmonic generation from planar photonic crystal," Opt. Lett. **28**, 2500–2502 (2003).
10. A. R. Cowan and J. F. Young, "Mode matching for second-harmonic in photonic crystal waveguides," Phys. Rev. B **65**, 085105 (2002).
11. B. R. Bennett, R. A. Soref, and J. A. D. Alamo, "Carrier-induced change in refractive index of InP, GaAs, and InGaAsP," IEEE J. Quantum Electron. **26**, 113–122 (1990).
12. M. G. Banaee, A. R. Cowan, and J. F Young, "Third-order nonlinear influence on the specular reflectivity of two-dimensional waveguide-based photonic crystals," J. Opt. Soc. Am. B **19**, 2224–2231 (2002).
13. A. R. Cowan, P. Paddon, V. Pacradouni, and J. F. Young, "Resonant scattering and mode coupling in two-dimensional textured planar waveguides," J. Opt. Soc. Am. A **18**, 1160–1170 (2001).
14. F. Sfigakis, P. Paddon, V. Pacradouni, M. Adamcyk, C. Nicoll, A. R. Cowan, T. Tiedje, and J. F. Young, "Near-infrared refractive index of thick, laterally oxidized AlGaAs cladding layers," J. Lightwave Technol. **18**, 199–202 (2000).
15. R. W. Boyd, *Nonlinear Optics* (Academic, 1992).
16. M. Sheik-Bahae, J. Wang, and E. W. Van Stryland, "Nondegenerate optical Kerr effect in semiconductors," IEEE J. Quantum Electron. **30**, 249–255 (1994).
17. G. I. Stegeman, M. Sheik-Bahae, E. Van Stryland, and G. Assanto, "Large nonlinear phase shifts in second-order nonlinear-optical processes," Opt. Lett. **18**, 13–15 (1993).
18. J. Talghader and J. S. Smith, "Thermal dependence of the refractive index of GaAs and AlAs measured using semiconductor multilayer optical cavities," Appl. Phys. Lett. **66**, 335–337 (1995).
19. D. M. Whittaker and I. S. Culshaw, "Scattering-matrix treatment of patterned multi-layer photonic structures," Phys. Rev. B **60**, 2610–2618 (1999).
20. T. S. Sosnowski, T. B. Norris, H. H. Wang, P. Grenier, J. F. Whitaker, and C. Y. Sung, "High-carrier-density electron dynamics in low-temperature-grown GaAs," Appl. Phys. Lett. **70**, 3245–3247 (1997).
21. C. Aversa, J. E. Sipe, M. Sheik-Bahae, and E. W. V. Stryland, "Third-order optical nonlinearities in semiconductors: the two-band model," Phys. Rev. B **50**, 18073–18082 (1994).
22. H. W. Tan, J. E. Sipe, H. M. van Driel, S. L. Schweizer, J. Schilling, and R. B. Wehrspohn, "Influence of mode characteristics on optical tuning of a two-dimensional silicon photonic crystal," Phys. Rev. B (submitted for publication).